Preprint typeset in JHEP style - HYPER VERSION

LU-TP 05-11
hep-ph/0503293

W+jets Matrix Elements and the Dipole Cascade

Nils Lavesson and Leif Lönnblad

Dept. of Theoretical Physics, Sölvegatan 14A, S-223 62 Lund, Sweden
E-mail: Nils.Lavesson@thep.lu.se *and* Leif.Lonnblad@thep.lu.se

Abstract: We extend the algorithm for matching fixed-order tree-level matrix element generators with the Dipole Cascade Model in Ariadne to apply to processes with incoming hadrons. We test the algoritm on for the process W+n jets at the Tevatron, and find that the results are fairly insensitive to the cutoff used to regularize the soft and collinear divergencies in the tree-level matrix elements. We also investigate a few observables to check the sensitivity to the matrix element correction.

Keywords: QCD, Jets, Parton Model, Phenomenological Models.

Contents

1. Introduction **1**

2. CKKW **3**
- 2.1 The original CKKW procedure 5
- 2.2 CKKW in hadronic collisions 6

3. The Dipole Cascade Model **7**
- 3.1 ARIADNE and CKKW 8
- 3.2 The Dipole Cascade Model for Incoming Hadrons 9
- 3.3 Gluon emission from an extended source 9
- 3.4 Sea-quark emissions from remnant dipoles 11

4. ARIADNE and CKKW for W production **12**
- 4.1 Constructing the Emissions 13
- 4.2 Reweighting the Events 14
- 4.3 The Full Algorithm 16

5. Results **16**

6. Conclusions **23**

A. Appendix: Construction **26**

1. Introduction

Parton Shower based Monte Carlo Event Generators (PSEGs) have developed into essential tools in High Energy Physics. Without them it is questionable if it at all would be possible to embark on large-scale experiments such as the LHC. Although they are based on leading logarithmic approximations and phenomenological hadronization models, they are typically able to describe hadronic final states in great detail and, especially at LEP, with great precision. However, there are problems. The description of final states which include more than three hard jets is not very good, and when it comes to collisions with incoming hadrons, the precision is generally lacking, especially for small-x processes. In this article we will address both these problems.

The problem with describing several hard, well separated jets is inherent in the leading log approximations, since they assume that there is strong ordering between parton emissions, and hence only give a good description of soft inter-jet and collinear intra-jet emissions. Typically it is possible to correctly describe one additional hard jet on top of

the hard sub-process used as starting point, by applying correction factors to the basic splitting functions. However, to go beyond one additional jet is more difficult.

To describe events with several hard partons we can use so-called Matrix Element Generators (MEGs), where the parton distributions can be generated according to exact tree-level matrix elements. Unfortunately these matrix elements are divergent in the soft and collinear limits and a cutoff is needed to avoid these regions of phase space. However, to generate realistic events we need to hadronize the partons into jets of hadrons, and all reasonable hadronization models require that also soft and collinear parton emissions are modeled correctly. Hence the need for combining matrix element generators with parton showers.

Combining these two approaches is, however, not trivial. The matrix elements describe inclusive events, ie. events with at least n partons above some cutoff, while parton showers are exclusive and describe events with exactly n partons. Naively adding parton showers to events generated by a MEG will therefore give a very strong dependence on the cutoff used in the MEG, even if great care is taken to avoid double-counting by only adding parton showers below that cutoff.

A solution for this problem was presented by Catani et al. in [1]. The procedure, generally referred to as CKKW, relies on applying a jet clustering algorithm to partonic event from a MEG generating zero, one, two, etc. additional hard jets above some cutoff according to exact tree-level matrix elements. The repeated clustering of two jets into one is then used to construct an ordered set of scales corresponding to consecutive parton emissions. These scales are used to calculate Sudakov form factors corresponding to no-emission probabilities, which are used to reweight the MEG events to make them exclusive. A parton shower can then be added with a special veto to avoid double-counting of emissions above the cutoff. In this way it was shown that the dependence on the cutoff cancels to next-to-leading order accuracy. The dependence was, however, still quite visible, giving rise to annoying discontinuities in some observables.

The basic CKKW prescription was somewhat improved [2] when implemented for the Dipole Cascade model [3,4] in the ARIADNE program [5]. Rather than using a jet clustering algorithm to construct a set of scales, the ARIADNE procedure involves constructing complete intermediate states corresponding to a series of emissions which the dipole cascade could have used to produce a given state obtained from a MEG. A special veto algorithm is used to calculate exactly the Sudakov form factors the cascade would have used to produce the state, which are then used for reweighting. In addition a special treatment of the MEG-produced states with highest multiplicity was introduced, avoiding the restriction which disallowed additional jets above the cutoff in the original CKKW paper. It should be noted that both these improvements are of "cosmetic" nature, in that the cutoff dependence is still formally only canceled to next-to-leading order accuracy.

Both these procedures were originally developed for e^+e^-. Recently there has been some developments in applying them to hadronic collisions, in particular for the W+jets process, by Krauss et al. [6–8] and Mrenna and Richardson [9]. An alternative procedure has also been developed by Mangano [10, 11], which is similar in spirit to CKKW, but which has a simpler interface between the MEG and PSEG. This development is very

important for the LHC, where W+jets is an important background for almost any signal of new physics.

In this article we describe the extension of the CKKW procedure for the dipole cascade in ARIADNE to handle hadronic collisions, again concentrating on the W+jets process. The goal is to obtain a procedure which gives as small cutoff dependence as was achieved for e^+e^-. However, we also expect to see differences w.r.t. the procedures of Mrenna, Richardson and Krauss, since the dipole cascade model for collisions with incoming hadrons [12, 13] is different. The standard initial-state parton shower approaches, such as those implemented in PYTHIA [14, 15], HERWIG [16] and SHERPA/APACIC++ [17, 18], as well as the Sudakov form factors used in CKKW, correspond to a DGLAP-resummation [19–22] of leading logarithms of the hard scale. In the dipole cascade, however, also some terms corresponding to logarithms of $1/x$ are resummed. Although not formally equivalent to neither BFKL [23–25] or CCFM [26–29] evolution, it has proven to be able to describe most features small-x final states at HERA, where all DGLAP-based parton showers fail. Now, W+jets is conventionally not considered to be a small-x process because of the hard scale, m_{W}, being large, but at the LHC the collision energies are so large there may be substantial effects of terms proportional to $\alpha_{\mathrm{s}}^n \log(\sqrt{S}/m_{\mathrm{W}})^n$, where $m_{\mathrm{W}}/\sqrt{S} \sim x \sim 0.005$.

The layout of this article is as follows. We will first recap the main points of the CKKW procedure in section 2. Then, in section 3, we describe the dipole cascade model and CKKW implementation for e^+e^- annihilation, followed by a description of the dipole cascade for incoming hadrons in section 3.2. In section 4 we will describe our CKKW implementation for W+jets, and hadronic collisions in general, starting with the construction of intermediate states in 4.1, followed by the reweighting procedure in 4.2. The results of our investigation of its performance are presented in 5. Finally in section 6 we present our conclusions.

2. CKKW

When generating events with a PSEG, the procedure is to start from a primary hard sub-process, typically a $2 \to 2$ process such as $e^+e^- \to q\bar{q}$ or $q\bar{q} \to \mathrm{W} \to \bar{\nu}e$, and then to let the incoming and outgoing quarks and gluons evolve a parton cascade in an iterative $1 \to 2$ branching procedure. The emissions are ordered according to some evolution scale ρ, where the maximum scale, ρ_0 is typically given by the hardest scale in the primary sub-process, and the minimum is some cutoff scale of the order of one GeV, typically tuned to match a particular hadronization model.

We can write the exclusive cross sections for in this way generating 0, 1, 2, ... additional partons above the cutoff, ρ_c, as

$$\begin{aligned}
\sigma_{+0} &= \sigma_0\, \Delta_{S_0}(\rho_0, \rho_c) \\
d\sigma_{+1} &= \sigma_0\, \alpha_{\mathrm{s}}(\rho_1) c_{11}^{\mathrm{PS}} \Delta_{S_0}(\rho_0, \rho_1) \Delta_{S_1}(\rho_1, \rho_c) d\rho_1 d\Omega_1 \\
d\sigma_{+2} &= \sigma_0\, \alpha_{\mathrm{s}}(\rho_1)\alpha_{\mathrm{s}}(\rho_2) c_{22}^{\mathrm{PS}} \Delta_{S_0}(\rho_0, \rho_1) \Delta_{S_1}(\rho_1, \rho_2) \Delta_{S_2}(\rho_2, \rho_c) d\rho_1 d\Omega_1 d\rho_2 d\Omega_2 \\
&\vdots
\end{aligned}$$

$$
\begin{aligned}
d\sigma_{+n} &= \sigma_0\, c^{\mathrm{PS}}_{nn}\Delta_{S_n}(\rho_n,\rho_c)\prod_{i=1}^{n}\alpha_{\mathrm{s}}(\rho_i)\Delta_{S_{i-1}}(\rho_{i-1},\rho_i)d\rho_i d\Omega_i \\
&\vdots
\end{aligned}
\tag{2.1}
$$

where the ordering is $\rho_0 > \rho_1 > \ldots > \rho_n > \rho_c$ and Ω_i symbolizes the phase space variables defining the ith emission in addition to ρ_i (typically some momentum fraction, z_i, and some azimuth angle ϕ_i). $\Delta_{S_i}(\rho_i,\rho_{i+1})$ is the so-called Sudakov form factor giving the probability that no emissions occurred from the state with i additional partons between the scales ρ_i and ρ_{i+1}. The coefficients c^{PS}_{nn} are basically products of splitting functions which depends on ρ_i and Ω_i, and we assume an implicit sum over all possible flavour combinations. As we will see below, the c^{PS}_{nn} may also include ratios of parton density functions (PDFs) in the case of incoming hadrons.

The Sudakov form factors are formally resummations of virtual diagrams to all orders and can, in principle, be calculated analytically. They would then only depend on the limiting scales, as is done in the standard CKKW procedure. However, when explicitly interpreted as a no-emission probability in a PSEG, as is done eg. in ARIADNE, it basically depends on all momenta in the partonic state. The typical form of the Sudakov is

$$
\Delta_S(\rho_i,\rho_{i+1}) = \exp\left(-\int_{\rho_{i+1}}^{\rho_i}\frac{d\rho}{\rho}\alpha_{\mathrm{s}}(\rho)\int dz P(z)\right), \tag{2.2}
$$

which, of course, can be expanded in a series in α_{s}, and we can rewrite the exclusive cross sections as

$$
\begin{aligned}
\sigma_{+0} &= \sigma_0\,(1 + c^{\mathrm{PS}}_{01}\alpha_{\mathrm{s}} + c^{\mathrm{PS}}_{02}\alpha_{\mathrm{s}}^2 + \ldots) \\
d\sigma_{+1} &= \sigma_0\,\alpha_{\mathrm{s}}c^{\mathrm{PS}}_{11}(1 + c^{\mathrm{PS}}_{12}\alpha_{\mathrm{s}} + c^{\mathrm{PS}}_{13}\alpha_{\mathrm{s}}^2 + \ldots)d\rho_1 d\Omega_1 \\
d\sigma_{+2} &= \sigma_0\,\alpha_{\mathrm{s}}^2c^{\mathrm{PS}}_{22}(1 + c^{\mathrm{PS}}_{23}\alpha_{\mathrm{s}} + c^{\mathrm{PS}}_{24}\alpha_{\mathrm{s}}^2 + \ldots)d\rho_1 d\Omega_1 d\rho_2 d\Omega_2 \\
&\vdots \\
d\sigma_{+n} &= \sigma_0\,\alpha_{\mathrm{s}}^n c^{\mathrm{PS}}_{nn}(1 + c^{\mathrm{PS}}_{n,n+1}\alpha_{\mathrm{s}} + c^{\mathrm{PS}}_{n,n+2}\alpha_{\mathrm{s}}^2 + \ldots)\prod_{i=1}^{n} d\rho_i d\Omega_i \\
&\vdots
\end{aligned}
\tag{2.3}
$$

to emphasize the resummation aspect. We note that even though all the coefficients c^{PS}_{ij} are divergent in the soft and collinear limit when $\rho_c \to 0$, the resummation to all orders in the Sudakovs gives a finite result for each of the cross sections. Also, when integrated over the allowed phase space the cross section of the primary sub process σ_0 is retained,

$$
\sum_0^\infty \sigma_{+i} = \sigma_0. \tag{2.4}
$$

In contrast a MEG will generate inclusive partonic states with the cross sections for generating *at least* 0, 1, 2, ... additional jets given by

$$
\begin{aligned}
\sigma_{+0} &= \sigma_0 \\
d\sigma_{+1} &= \sigma_0\, \alpha_{\mathrm{s}} c_{11}^{\mathrm{ME}} d\mathbf{\Omega}_1 \\
d\sigma_{+2} &= \sigma_0\, \alpha_{\mathrm{s}}^2 c_{22}^{\mathrm{ME}} d\mathbf{\Omega}_1 d\mathbf{\Omega}_2 \\
&\vdots \\
d\sigma_{+n} &= \sigma_0\, \alpha_{\mathrm{s}}^n c_{nn}^{\mathrm{ME}} \prod_{i=1}^{n} d\mathbf{\Omega}_i \\
&\vdots
\end{aligned}
\tag{2.5}
$$

where the $\mathbf{\Omega}_i$ symbolizes all phase space variables defining the ith parton, and the coefficients c_{ii}^{ME} are calculated using the exact tree-level matrix elements (including PDFs in the case of incoming hadrons). Clearly we can not simply add these cross sections, especially since each of the coefficients are divergent if the soft and collinear limits are not cut off properly.

The advantage of using a MEG is that the exact tree-level matrix elements are used, which means that also states with several hard partons are described correctly. This is not the case for the PSEG, where the coefficients are given by products of splitting functions, which is only a good approximation in the limit of strongly ordered emissions. On the other hand a MEG will not correctly treat soft and collinear partons, where the coefficients are large and need to be resummed to all orders, as in a PSEG, to give reliable results. Clearly it would be highly desirable to combine the two approaches.

It should be noted that for the first emission in a PSEG is typically quite easy to modify the splitting functions to correctly reproduce the exact matrix element, effectively replacing c_{11}^{PS} with c_{11}^{ME}, and in most PSEGs this is the default behavior for most primary sub-processes [3, 5, 13, 30–38].

2.1 The original CKKW procedure

Comparing eqs. 2.1 and 2.5 the solution should be obvious. Use a MEG to generate up to N additional partons above some cutoff, y_{cut}, but reweight the generated states with the Sudakov form factors, and then add a parton shower with the requirement that no partons above y_{cut} are emitted. This is the essence of the CKKW procedure. To calculate the Sudakov form factors we need an ordered set of emission scales, which is not provided by the MEG, since there all possible diagrams are added coherently and emission scales are not well defined. In the original CKKW procedure, the $k_\perp$clustering algorithm [39, 40] was used to define an ordered set of scales which were used to analytically calculate the Sudakov form factors. A reweighting was also done to use a running $\alpha_{\mathrm{s}}$with the constructed scale as argument. The resolution variable of the $k_\perp$-algorithm was also used for the cutoff in the MEG, which is not the same as the evolution variable in the PSEG. To ensure a full coverage of the phase space the parton shower was therefore added with the maximum scale as starting point, but vetoing all emissions corresponding to the $k_\perp$-algorithm resolution variable above y_{cut} to avoid double-counting.

It was shown that this procedure removes the dependence on the MEG cutoff, $y_{\rm cut}$, to next-to-leading logarithmic accuracy. However, there was still a clearly visible discontinuity in some generated distributions.

2.2 CKKW in hadronic collisions

To extend this algorithm to be used for hadronic collisions is conceptually straight forward. In [7] and [9] the standard CKKW procedure was extended to hadronic collisions in general and for the W+jets process in particular, and implemented for the APACIC++, HERWIG and PYTHIA PSEGs. The principle is the same as for e^+e^-. Jet construction is done with the $k_\perp$-algorithm modified for hadronic collisions according to [41]. The resulting ordered set of scales is used in the analytic Sudakov form factors (in [9] a Sudakov veto algorithm similar to the one in ARIADNE was used for the PYTHIA implementation), and the events from the MEG was reweighted with these and the properly scaled $\alpha_{\rm s}$. The MEG states with highest multiplicity was treated in the same way as in the ARIADNE implementation above.

There are some issues which need to be treated with special care. In a PSEG, the initial states emissions are generated in a backward evolution procedure which besides the standard partonic splitting functions also involves ratios of PDFs. The leading order cross section is given by

$$d\sigma_0 = d\sigma_{hh\to \rm W} = \sum_{\rm q,q'} x f_{\rm q}(x_+,\mu^2) x f_{\rm q'}(x_-,\mu^2)\hat{\sigma}_{\rm qq'\to W}(x_+x_-S)\frac{dx_+}{x_+}\frac{dx_-}{x_-}, \qquad (2.6)$$

where the scale $\mu^2 = m_{\rm W}^2 = x_+x_-S$. Making one step in the backward evolution with a $\rm g \to q\bar{q}$ splitting will be performed with a probability

$$dP(Q^2,z) = \alpha_{\rm s}P_{\rm g\to q}(z)\frac{\frac{x_+}{z}f_{\rm g}(\frac{x_+}{z},Q^2)}{x_+f_{\rm q}(x_+,Q^2)}\Delta_S(Q^2_{\rm max},Q^2)\frac{dQ^2}{Q^2}dz, \qquad (2.7)$$

where the Sudakov form factor can be formulated both with (PYTHIA) and without (HERWIG) ratios of PDFs. Both choices are formally equivalent in the leading-log approximation, but only the former choice corresponds exactly to a no-emission probability. The maximum scale is typically given by $m_{\rm W}^2$, and the Sudakov form factor corresponds to a leading-log DGLAP resummation[1]. However, clearly there is nothing in the real world preventing emissions with a scale above $m_{\rm W}^2$, and such parton states will be generated by the MEG. In [7] states with one or more partons emitted at a scale above $m_{\rm W}^2$ are treated as coming from a separate class of primary sub-processes, and the Sudakov form factors are added only for additional emissions with a maximum scale given by the smallest of the constructed scales above $m_{\rm W}^2$.

Although the resulting procedures in [7] and [9] are shown to be fairly cutoff insensitive, there is still some dependence, and it may be worth while to extend also the ARIADNE implementation of CKKW to hadronic collisions to see if a better result can be achieved.

[1] Also next-to-leading logarithmic Sudakov form factors may be used [1], although these may become larger than unity, disabling the interpretation as no-emission probabilities.

As for the standard CKKW this extension is in principle straight forward. However, there are some tricky issues, mainly to do with the treatment of parton densities, and to describe how we deal with these, we first have to describe how hadronic collisions are implemented in ARIADNE.

3. The Dipole Cascade Model

ARIADNE implements the dipole cascade model which is quite different from conventional parton cascades. Rather than iterating $1 \to 2$ parton splittings, gluons are emitted from colour-dipoles between colour-connected partons resulting in $2 \to 3$ parton splittings. This model has several advantages. Since gluons are emitted coherently by colour-connected partons, there is no need for explicit angular ordering. In addition, the evolution variable is defined as a Lorentz-invariant transverse momentum which also is a suitable scale to be used in α_s. The evolution variable is defined as (for massless partons)

$$p_\perp^2 = \frac{s_{12}s_{23}}{s_{123}}, \tag{3.1}$$

where parton 2 is the emitted one and s_{ij} and s_{ijk} are the squared invariant masses of the two- and three-parton combinations.

The probability for an emission is given in terms of the dipole splitting functions, which depend on $p_\perp^2$ and a Lorentz invariant rapidity defined as

$$y = \frac{1}{2}\ln\frac{s_{12}}{s_{23}}. \tag{3.2}$$

The probability of a gluon emission from a dipole between two partons i, j is then given by

$$dP(p_\perp^2, y) = \alpha_s(p_\perp^2) D_{ij}(p_\perp^2, y) \exp\left(-\int_{p_\perp^2} \frac{dp_\perp'^2}{p_\perp'^2}\int dy' \alpha_s(p_\perp'^2) D_{ij}(p_\perp'^2, y')\right) \frac{dp_\perp^2}{p_\perp^2} dy, \tag{3.3}$$

where $\exp(\ldots)$ is the Sudakov form factor. The dipole splitting functions, D_{ij}, depends on which partons are involved according to

$$D_{q\bar{q}}(p_\perp^2, y) = \frac{2}{3\pi}\frac{x_1^2 + x_3^2}{(1-x_1)(1-x_3)} \tag{3.4}$$

$$D_{qg}(p_\perp^2, y) = \frac{3}{4\pi}\frac{x_1^2 + x_3^3}{(1-x_1)(1-x_3)} \tag{3.5}$$

$$D_{gg}(p_\perp^2, y) = \frac{3}{4\pi}\frac{x_1^3 + x_3^3}{(1-x_1)(1-x_3)} \tag{3.6}$$

where x_i are the resulting energy fractions of the emitting partons in the original dipole rest system, $x_i = 2E_i/\sqrt{s_{123}}$, related to $p_\perp^2$ and y according to

$$y = \frac{1}{2}\ln\left(\frac{1-x_3}{1-x_1}\right), \qquad p_\perp^2 = s_{123}(1-x_1)(1-x_3). \tag{3.7}$$

It can be shown that the dipole splitting functions are equivalent to the standard Altarelli–Parisi splitting functions in the relevant soft and collinear limits [3]. We also note that the $D_{q\bar{q}}$ exactly corresponds to the leading order $e^+e^- \to qg\bar{q}$ tree-level matrix element.

Another feature of the dipole cascade, which will turn out to be important for the CKKW implementation, is that all partons are always on shell throughout the cascade. This is possible since the recoil from the emitted parton can be absorbed by the two emitting ones. In contrast, a conventional parton cascade does not have on-shell intermediate states, and the full kinematics of an event is not constructed until all the scales in the complete shower have been generated. While the energy loss of the emitting partons are defined in the splitting functions in eqs. (3.4)–(3.6), the transverse recoil is chosen according to principles detailed in [5].

It can be noted that the "inverse" of the dipole cascade is a well-behaved jet clustering algorithm. In fact such an algorithm has been constructed, the DICLUS algorithm [42], based on successive clusterings of three jets into two, using the $p_\perp$in eq. (3.1) as resolution scale, which has been shown to have many attractive features [43].

There are, however, also some disadvantages with the dipole cascade model, the main one being that it only deals with gluon emissions, and the splitting of gluons into $q\bar{q}$ pairs must be added by hand, both for final-state [44] and initial-state [35] splitting.

The initial-state splitting will be described in section 3.4 below. Final-state splittings are simply added as a possibility for a dipole connected to a gluon to split this gluon into a $q\bar{q}$-pair in addition to emit a gluon. Here, the standard Altarelli–Parisi splitting function is used, divided between the two dipoles connected to the gluon. This will result in a new dipole splitting function,

$$D_{ig}^{q\bar{q}} = \frac{\xi}{4\pi}\frac{(1-x_2)^2+(1-x_3)^2}{1-x_1}. \tag{3.8}$$

In the original formulation, the splitting was divided equally between the two dipoles connected to the gluon, ie. $\xi = 0.5$. However, in the current ARIADNE implementation, a larger fraction is given to the smaller of the dipoles ig and gj, hence for the ig dipole we have $\xi = s_{gj}/(s_{gj}+s_{ig})$.

Although these splitting do not come in naturally in the dipole picture, they can be incorporated in a consistent way and the resulting implementation in ARIADNE is probably the best model for describing both e^+e^- final states at LEP [45], and DIS final states at HERA [46].

3.1 ARIADNE and CKKW

The ARIADNE implementation of CKKW for e^+e^- is described in detail in [2]. Considering the nature of the dipole cascade it may seem reasonable to use the dipole clustering algorithm in DICLUS to construct scales, rather than using the $k_\perp$-algorithm. However, in the ARIADNE implementation a step further is taken. For each partonic state generated by a MEG, all possible dipole cascade histories are constructed, basically answering the question *how would ARIADNE have generated this state?* A specific history is then picked by weighting possible histories with the product of the corresponding dipole splitting functions. The implementation depends on the MEG generating specific colour connections among the partons. Although this information is not physical, it is usually provided by MEG programs. (See discussion in ref. [47]). In principle one could choose between all

possible colour connections in the same way as different histories are considered, but as most MEGs supply colour information this is not necessary.

From a MEG generated state with n additional partons, we can construct, not only an ordered set of emission scales, $p^2_{\perp n}, p^2_{\perp n-1}, \ldots p^2_{\perp 1}$, but also the corresponding set of intermediate states, $S_{n-1}, S_{n-2}, \ldots S_0$. As in the standard CKKW, the reweighting with the correct scales in α_s is done using just the constructed scales. However, the Sudakov form factors are calculated using the fact that $\Delta_{S_i}(p^2_{\perp i}, p^2_{\perp i+1})$ exactly corresponds to the probability that no emission occurred from state S_i between the scales $p^2_{\perp i}$ and $p^2_{\perp i+1}$. Hence, letting ARIADNE make a trial emission, starting from the state S_i with $p^2_{\perp i}$ as the maximum scale and throwing away the MEG event if the trial emission was above $p^2_{\perp i+1}$, will exactly correspond to reweighting with the same Sudakov form factor, $\Delta_{S_i}(p^2_{\perp i}, p^2_{\perp i+1})$, which ARIADNE would have used when generating the event.

A special treatment is given the trial emission from the MEG generated state, S_n. Rather than using the cutoff, $p^2_{\perp c}$, from the dipole cascade, the event is thrown if the emission is above the cutoff used in the MEG, while if the emission is below, the emission is kept and the cascade is continued down to $p^2_{\perp c}$ to produce a full ME+PS event. In addition, if $n = N$, the highest number of additional partons generated from the MEG, the emission from S_N is always kept. This was not done in the original CKKW prescription, but is clearly needed, since otherwise we would never get events with $N + 1$ additional partons above the cutoff. In later developments of CKKW such a treatment has been added [7, 9, 48].

3.2 The Dipole Cascade Model for Incoming Hadrons

In contrast to conventional parton shower models, the dipole cascade model does not separate between initial- and final-state gluon radiation. Instead, gluons are always emitted from final-state dipoles as in the e^+e^- case. The cleanest situation is in the DIS electroproduction case, where the leading order process is eq $\rightarrow$ eq, ie. a quark is being kicked out of a hadron. A gluon may then be emitted from the colour-dipole between the struck quark and the hadron remnant, using the same dipole splitting function as in the e^+e^- case in eq. (3.4). There is one major difference though. In the e^+e^- case, both the quark and anti-quark can be considered point-like, but in the DIS case only the struck quark is point-like (at least up to the resolution scale, Q^2, of the exchanged virtual photon) while the hadron remnant is an extended object with a size of roughly one fermi. Just as for the electromagnetic case, radiation of wavelengths much smaller than the size of the antenna is suppressed.

3.3 Gluon emission from an extended source

In [12] it was argued that only a fraction of the hadron remnant is effectively taking part in the emission. For a gluon emission at the scale $p^2_\perp$ this fraction is given by

$$a(p_\perp) = \left(\frac{\mu}{p_\perp}\right)^\alpha, \tag{3.9}$$

where μ parameterizes the inverse size of the remnant and α reflects the dimensionality of the emitter. If only that fraction of the remnant momentum is allowed to take part in the emissions, this corresponds to a sharp cut in the allowed phase space for gluon emission, limiting the transverse momentum mainly in the remnant direction according to

$$p_\perp < \frac{Wa(p_\perp)}{e^{+y} + a(p_\perp)e^{-y}}. \tag{3.10}$$

Here we note another major difference as compared to conventional initial-state parton showers. From eq. (3.10) it is easy to see that the maximum scale is given by

$$p_{\perp\max} = \left(\frac{W^2\mu^\alpha}{4}\right)^{\frac{1}{2+\alpha}}, \tag{3.11}$$

which may be much larger than Q^2 which is used as the maximum scale in conventional PSEGs, especially for small x values since $W^2 \approx Q^2/x$. Since the maximum scale is also used in the Sudakov form factors, these do not only correspond to a standard DGLAP resummation of leading logarithms of Q^2, but in the dipole model they also resum, at least partially, logarithms of $1/x$. Note however, that there is no formal equivalence to BFKL or CCFM evolution. There is another similarity though. Even though the emissions in the dipole model are ordered in $p_\perp$, they are not ordered in rapidity, and conversely, following the emissions in rapidity from the struck quark the transverse momenta of the gluons will be unordered as in BFKL and CCFM.

In the implementation in ARIADNE, the sharp cutoff in $p_\perp$is replaced by a smooth function, $\Theta(p_\perp^2, y)$, with some power suppression for emissions violating eq. (3.10). Concentrating on the soft and collinear limits, where the splitting function is simply $\propto d\ln p_\perp^2 dy$, we can write the probability of emitting a gluon as

$$dP(p_\perp^2, y) = \frac{4\alpha_s}{3\pi}\Theta(p_\perp^2, y)\Delta_S(W^2, p_\perp^2)\frac{dp_\perp^2}{p_\perp^2}dy \tag{3.12}$$

Comparing this to the corresponding initial-state $q \to q$ splitting in a conventional parton shower, (cf. eq. (2.7)) where we have

$$dP(Q^2, z) = \frac{4\alpha_s}{3\pi}\frac{1}{1-z}\frac{\frac{x_+}{z}f_q(\frac{x_+}{z}, Q^2)}{x_+ f_q(x_+, Q^2)}\Delta_S(Q^2_{\max}, Q^2)\frac{dQ^2}{Q^2}dz, \tag{3.13}$$

and noting that in this limit

$$\frac{1}{z(1-z)}\frac{dQ^2}{Q^2}dz = \frac{dp_\perp^2}{p_\perp^2}dy, \tag{3.14}$$

we see that the suppression function, Θ, corresponds to the ratio of PDFs

$$\Theta(p_\perp^2, y) \to z\frac{\frac{x_+}{z}f_q(\frac{x_+}{z}, Q^2)}{x_+ f_q(x_+, Q^2)} \tag{3.15}$$

The fact that only a part of the remnant takes part in a gluon radiation also means that only a fraction of it will obtain a transverse recoil in an emission. This is handled by

the addition of so-called recoil gluons and is described in some detail in [5]. These recoil gluons will not be relevant for this report, however they will play a role when implementing CKKW in ARIADNE for DIS and we will come back to them in more detail in a future publication [49].

For W production in hadronic collisions, the primary sub-process is $q\bar{q} \to W$ and the initial dipole from which gluons are radiated is between the two remnants. The model is now the same as in DIS. However, since both remnants are extended, the cutoff in eq. (3.10) becomes

$$p_\perp < \frac{W a_1(p_\perp) a_2(p_\perp)}{a_2(p_\perp) e^{+y} + a_1(p_\perp) e^{-y}}, \tag{3.16}$$

and the maximum scale is

$$p_{\perp\max} = \left(\frac{W^2 \mu_1^{\alpha_1} \mu_2^{\alpha_2}}{4} \right)^{\frac{1}{2+\alpha_1+\alpha_2}}. \tag{3.17}$$

Again the sharp cutoff is replaced by a power suppression of transverse momenta above the limit in eq. (3.16). Rather than introducing recoil gluons to absorb the transverse recoil, we note that any emission from the primary dipole corresponds to initial-state radiation, for which it is natural that the recoil is taken by the W (otherwise it would not be possible to produce a W with non-zero transverse momentum). In [13] the choice was to always transfer the transverse recoil to the W in the first emission, while in subsequent emissions, the recoil is only transferred if the emitted gluon is close to the W in phase space.

3.4 Sea-quark emissions from remnant dipoles

Besides gluon radiation, there is also a possibility that one of the quarks fusing into the W is a sea-quark, in which case it could have come from a perturbative splitting of a gluon as in eq. (2.7). As for the final-state gluon splitting into $q\bar{q}$, this process does not come in naturally in the dipole model. Instead it is added by hand as an explicit initial-state splitting. This procedure is detailed in [35], and is based on different treatments of the remnants depending on whether a valence- or a sea-quark entered into the primary sub-process. A sea-quark is picked with the probability $xf_{sq}(x,Q^2)/(xf_{sq}(x,Q^2)+xf_{vq}(x,Q^2))$ and in this case the complex remnant containing the anti-sea-quark and the valence quarks is split into a colour-singlet hadron containing the anti-sea-quark and a simple remnant. The sharing of longitudinal momentum is inspired by the string fragmentation function as explained in detail in [12]. A dipole connected to such a remnant is now allowed to emit the anti-sea-quark in a way similar to a standard initial-state parton shower, except that the ordering is in transverse momentum, changing eq. (2.7) to

$$dP(p_\perp^2, z) = \alpha_s P_{g\to q}(z) \frac{\frac{x_+}{z} f_g(\frac{x_+}{z}, p_\perp^2)}{x_+ f_q(x_+, p_\perp^2)} \Delta_S(p_{\perp\max}^2, p_\perp^2) \frac{dp_\perp^2}{p_\perp^2} dz. \tag{3.18}$$

As for the case of final-state gluon splitting, there is now in the W-production case several competing processes which can occur in the primary dipole, and after generating one emission of each, the one which gave the largest $p_\perp$ is chosen. If the emission of an anti-sea-quark is chosen, it will form a new dipole with the remnant of the hadron to which it

previously belonged. The transverse recoil is taken by hard subsystem, just as in a standard parton shower, where the hard subsystem in our case is the W and any other parton which has been previously emitted.

It may seem counterintuitive that the essentially non-perturbative splitting of the remnant is allowed to affect perturbative emissions. However, the splitting will mainly influence the region very close to the remnant, which is typically out of reach for current experiments. Nevertheless, we will investigate alternative treatments in a future publication.

Emitting an anti-sea-quark means that we have now extracted a gluon from the incoming hadron. In a standard parton shower scenario it would then be possible to evolve this gluon backwards either with a $g \to g$ splitting or a $q \to g$ splitting. In ARIADNE, the former is modeled by gluon emissions from either of the two dipoles connected to the two remnants. In this case we use the same suppression function as in eq. (3.12), but comparing to eq. (3.18) we find that it now corresponds to the ratio of gluon densities,

$$\Theta(p_\perp^2, y) \to \frac{\frac{x_+}{z} f_g(\frac{x_+}{z}, Q^2)}{x_+ f_g(x_+, Q^2)}, \tag{3.19}$$

where the extra factor z in eq. (3.15) is absent since this is now included in the gluon splitting function. The initial-state $q \to g$ splitting is not included in the ARIADNE program, but it could in principle be added in the same way as the sea-quark emission. Again we will investigate this in a future publication.

Clearly, the dipole model for incoming hadrons has some conceptual problems, especially when it comes to initial-state $g \to q$ splittings. However, it also has some advantages. The first emission is quite easily modified to correctly reproduce the leading order matrix element, both for DIS and W-production. Also, a larger part of phase space is available for gluon emissions as compared to DGLAP based initial-state parton showers. This enables ARIADNE to reproduce small-x observables in DIS, such as the forward jet rates, where no conventional shower succeeds. Below we shall also see that ARIADNE gives a somewhat harder peak in the W $p_\perp$-spectrum than conventional parton showers, which we know peaks below the data measured at the Tevatron.

Now that we have explained how ARIADNE handles W-production in hadronic collisions, we can proceed with describing how to combine it with a fixed-order tree-level MEG. As for the e^+e^- case it will involve constructing all possible cascade histories of a produced MEG state, the reweighting with Sudakov form factors using a Sudakov-veto algorithm, and finally the reweighting with α_s as well as with ratios of PDFs and the suppression function, Θ.

4. ARIADNE and CKKW for W production

The states delivered by a MEG contains information about the momenta, colour connections and types of the incoming and outgoing particles in the generated sub-process. The states are generated according to exact tree-level matrix elements, using a fixed α_s evaluated at some scale Q_0^2 and weighted by the relevant parton densities typically evaluated at the same scale. Q_0^2 is usually taken to be the cutoff scale used to regularize soft and collinear divergencies.

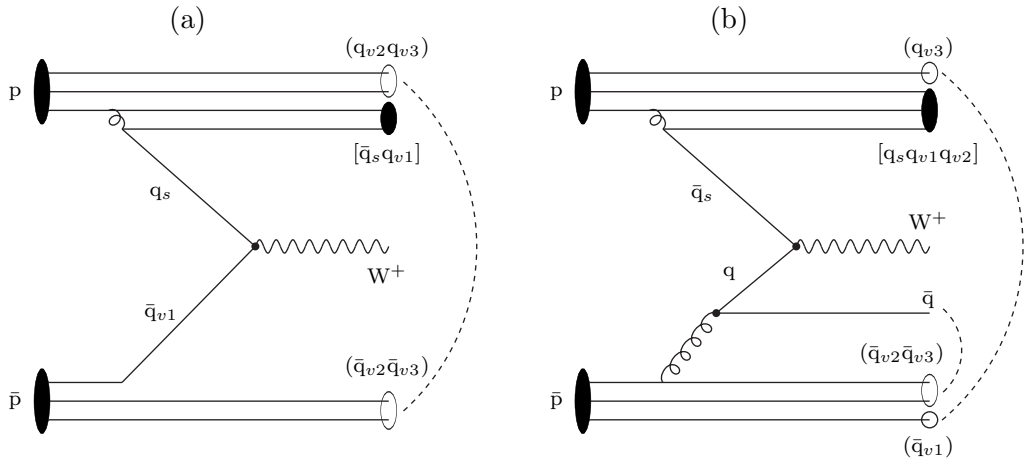

Figure 1: Different ways dipoles are connected (dashed arcs) depending on which kind of parton is extracted from a baryon. Filled ovals corresponds to colour-singlet hadrons, while open ovals represents coloured remnants.

4.1 Constructing the Emissions

To construct a dipole cascade history of this state it is first necessary to introduce the remnants so that all outgoing coloured particles from the sub-process are connected with dipoles. This is done in the same way as for standard ARIADNE. In figure 1 the different possible connections of dipoles to the remnants are described schematically for W-production in $p\bar{p}$ collisions. We see that if a gluon has been extracted from a baryon (lower part of figure 1b), there are two remnants one containing a quark connected to parton in the end of anti-colour line of the gluon, and one di-quark connected to the end of the colour line. Furthermore, if a sea-quark is extracted from a proton (upper part of figure 1a), the parton in the end of its colour line will be connected with a di-quark remnant, while the anti-sea-quark will form a hadron together with the remaining valence flavour, as described in section 3.4 above. Similarly, if an anti-sea-quark is extracted (upper part of figure 1b), the parton in the end of its colour line will be connected with a single quark remnant, while the sea-quark will form a hadron together with the remaining valence flavours. Finally if a valence quark is extracted (lower part of figure 1a), the remnant is a di-quark which is connected with the parton on the end of the colour line.

The construction will now proceed iteratively, with each step corresponding to the inverse of an emission in the dipole cascade. All possible constructions will be made, and afterwards one of them will be picked. In each of the construction steps we must determine

- the scale of the corresponding emission;
- the value of splitting function to be used to give different weights to different possible construction paths;
- the ratio of PDFs or the value of the suppression function which would have been used in the corresponding emission (which will be used to reweight the events);
- and way the momentum of the emitted parton is distributed among the emitters.

In the last point, there will usually be three partons constructed into two, which means that the total energy and momentum is always conserved with all partons staying on-shell.

However, the orientation of the final two partons in the rest system of the construction needs to be specified.

Some of the possible construction steps correspond to emissions from dipoles between partons from the hard sub-process, and these are the same as in e^+e^-. Then there is a group of construction steps which involve hadron remnants, which are particular to hadronic collisions in general and to W-production in particular. In appendix A we present a complete list of all possible construction steps

After the construction procedure we are normally left with several possible cascade histories. Most of these will end up in a zeroth order state containing only remnants and one W with no transverse momentum. There will be some diagrams generated by the MEG which never could have come from an ARIADNE cascade. One example is the initial-state $q \to g$ splitting discussed in the end of section 3.4, in which case the constructed state is accepted anyway. However, there are also diagrams, such as the one in figure 2, which could not be produced even by a conventional parton shower. In this case the construction is stopped before reaching the zeroth order state, and this state is then treated as a separate leading order process and the reweighting is only applied to additional partons (similarly to the treatment in [7] mentioned above).

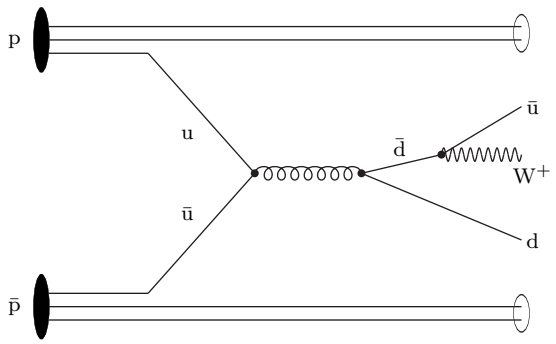

Figure 2: An example of a W-strahlung diagram. Such diagrams are not modeled by standard ARIADNE.

The resulting alternative cascade histories may or may not have an ordered set of constructed scales. When choosing a history according to their weights given by the products of the splitting functions, we first only consider true ARIADNE histories with ordered scales. Only if no such histories were found, the other histories are considered. Histories corresponding to figure 2 will only be considered if no full constructions are found.

4.2 Reweighting the Events

For a given MEG state, S_n, with n additional jets, we have now constructed a dipole cascade history with complete intermediate states, $S_n, \ldots, S_0$, and the corresponding emission scales, $p_{\perp n}, \ldots, p_{\perp 1}$, and we can proceed with the reweighting.

First we note that the MEG has used PDFs typically evaluated at the cutoff scale, Q_0^2 with x_+ and x_- given by the light-cone momentum fractions of the partons, i and j, entering the hard sub-process. This should be compared with the starting point for a normal parton cascade generation, where we just have a $q\bar{q}' \to W$ sub-process, and the PDFs are evaluated at the scale m_W^2 and x'_+ and x'_- given by the corresponding momentum fractions for the q and $\bar{q}'$. Our strategy is to follow the ARIADNE cascade as closely as possible, just replacing the product of dipole splitting function with the exact tree-level matrix element, so to get the same starting point, we take the q and $\bar{q}'$ of the state S_0 and their x'_+ and x'_-, and

reweight the event with

$$\omega_0 = \frac{x'_+ f_{\mathrm{q}}(x'_+, m^2_{\mathrm{W}}) \cdot x'_- f_{\bar{\mathrm{q}}'}(x'_-, m^2_{\mathrm{W}})}{x_+ f_i(x_+, Q_0^2) \cdot x_- f_j(x_-, Q_0^2)}. \tag{4.1}$$

If a construction instead ended in a state such as the one in figure 2, the corresponding incoming partons and their momentum fractions are used instead with the scale given by m_H^2, the squared invariant mass of the hard sub-process.

Then we reweight with all the PDF ratios, R_i^{PDF}, determined in the construction,

$$\omega_1 = \prod_{i=1}^{n} R_i^{\mathrm{PDF}}. \tag{4.2}$$

This comes about since the exact tree-level ME used corresponds to the product of splitting functions, while in a parton cascade we also have ratios of PDFs as in eqs. (3.13) and (3.18). Depending on the emission, these ratios can be either 1 for a final-state emission, the ratio of PDFs for the case of initial-state $\mathrm{q} \to \mathrm{g}$ and $\mathrm{g} \to \mathrm{q}$ splittings, the suppression function Θ for an initial-state $\mathrm{g} \to \mathrm{g}$ splitting and Θ/z for an initial-state $\mathrm{q} \to \mathrm{q}$ splitting (cf. eqs. (3.15) and (3.19)). We note that for a conventional parton cascade, where the Θ functions would be replaced by ratios of PDFs, the ω_0 and ω_1 weights would basically cancel each other, which is why these did not show up in the procedures in [7] and [9].

We then reweight with the correct scales in α_{s} according to

$$\omega_2 = \frac{\prod_{i=1}^{n} \alpha_{\mathrm{s}}(p^2_{\perp i})}{\alpha_{\mathrm{s}}(Q_0^2)^n}. \tag{4.3}$$

Again, for the situation in figure 2, the first two scales are taken to be m_H^2.

Finally we need to reweight with the Sudakov form factors in ARIADNE. This is done with the same Sudakov-veto algorithm as was presented in section 3.1. There are, however a few details which should be mentioned.

The starting scale for the trial emission from the leading order state, S_0, is given by $p^2_{\perp\max} = W^2/4$, where W is the total invariant mass of the hadronic collision, ie. the same as for the standard ARIADNE treatment of W production. For the situation in figure 2, m_H^2 is used instead.

If the constructed cascade history contains unordered scales, such that $p^2_{\perp i} < p^2_{\perp i+1}$, the two corresponding emissions will be treated as a combined emission with $p^2_{\perp i+1}$ as the scale. The Sudakovs will be generated with a trial emission from the state S_{i-1} with a minimum scale of $p^2_{\perp i+1}$ and a trial emission from the state S_{i+1} with a maximum scale of $p^2_{\perp i+1}$, while there is no Sudakov generated from the state S_i.

Finally, in the trial emission from the state S_n, for $n < N$, when checking if the resulting partons are above the jet cutoff used in the MEG, possible recoil gluons are not considered. Such recoil gluons may appear in ARIADNE, but they are typically rather soft, and including them would very often result in the emission being below the cutoff, even if the emitted gluon is not.

4.3 The Full Algorithm

We can now summarize the full algorithm. The way it is used below results in weighted events. This is because of the complicated reweightings which takes place. However, all weights are positive, and by carefully choosing the PDFs and α_s used in the MEG, it should be possible to have a vetoing procedure so that all events end up with unit weight.

1. First the number of partons, $n \leq N$, to be generated is chosen according to the integrated tree-level matrix elements in the MEG, using a cutoff Q_0^2 in the jet resolution scale given by the longitudinally invariant $k_\perp$-algorithm. A fixed α_s is used and the PDFs are typically sampled at the Q_0^2 scale.
2. Then the MEG is told to generate the momenta of the state with n additional partons according to the tree-level matrix element. Since we do not want any events below the cutoff in the dipole cascade, the invariant $p_\perp^2$ of the partons is checked, and if anyone is below $p_{\perp c}^2$, the state is rejected and the procedure is restarted at step 1.
3. Now, all the intermediate states $S_{n-1}, \ldots, S_0$ and scales $p_{\perp n}^2, \ldots, p_{\perp 1}^2$ are constructed according to the procedure in section 4.1, resulting in a possible dipole shower history of the generated S_n state.
4. The event is reweighted by the weight factors given in eqs. (4.1)–(4.3).
5. We now make a trial emission with the dipole cascade from the state S_0, starting from the maximum scale $p_{\perp\max}^2 = W^2/4$. If this emission is at a scale above $p_{\perp 1}^2$, the event is rejected and we restart from step 1. If not, a trial emission is performed from the state S_1 with a maximum scale of $p_{\perp 1}^2$. If this emission is at a scale above $p_{\perp 2}^2$ the event is rejected and we restart from step 1. This procedure is repeated for all states down to S_{n-1}. If no rejection has been made, a trial emission is made from the ME-generated state with n additional partons starting from the scale $p_{\perp n}^2$. There are now two cases
   (a) If $n = N$ the trial emission is always kept and the dipole cascade is allowed to continue down to the cutoff $p_{\perp c}^2$ and the event is accepted.
   (b) If $n < N$, and all parton pairs pass the cut, Q_0^2, used in the MEG, the event is rejected and we restart from step 1. If any of the partons fail the cut, the trial emission is accepted and the dipole cascade is allowed to continue down to the cutoff $p_{\perp c}^2$ and the event is accepted.

5. Results

To test our algorithm, we have generated $W^+ + n$jet events, with $n \leq N = 4$ with the MadGraph/MadEvent program [50] for a $p\bar{p}$ collider at a total energy of 1960 GeV, ie. corresponding to the Tevatron run II. The longitudinally invariant $k_\perp$-algorithm was used[2] to regularize the cross section, using cutoffs $E_{\text{cut}} = 12, 22$ and 50 GeV. We used the CTEQ6L [51] PDF parameterization using E_{cut}^2 as scale. E_{cut}^2 was also used as the

[2]Using `MODE=4211` in the KTClus program [41].

scale in α_s. The event was generated with unit weight and was then reweighted according to the algorithm in section 4.3. To avoid wildly fluctuating weights due to the ratios of PDFs, arising from situations in which the events in MADGRAPH had large x values where the PDF is very small, the W^+ was required to have limited rapidity, $|y| < 2.5$, and all partons were required to have a limited pseudorapidity, $|\eta| < 2.5$. For the same reason, when constructing the remnants, both the valence- and sea-quark alternatives were used with appropriate weights, rather than choosing between the two as described in section 3.4.

In the following we will use the notation MENPS for results from our new algorithm using W^++0,...,W^++N jets from MADGRAPH (the individual contributions from $W^+ + n$ jets are denoted ME$^n N$PS), while ARIADNE will denote results obtained with the default ARIADNE treatment.

As mention above, ARIADNE by default already has a matrix element correction for the first emission in W production[3]. Hence, as a first test of our new algorithm is to run it with $N = 1$, in which case we should get the same result as the standard default ARIADNE. In fact, had the construction procedure been exact, the results would be exactly the same. Of course, the construction can never be really exact, but for only one additional jet it is fairly close.

In figure 3 we show the $p_\perp$ spectrum of the W^+ for the new algorithm with $N = 1$, ME1PS, compared to default ARIADNE. Clearly the agreement is very good. In particular we note that there is no significant discontinuity or other strange behaviors around the different cutoffs used. This agreement is not trivial, since the ME1PS curve is a sum of W^++0 and W^++1 jet event from MADGRAPH. The fact that there is a small contribution of W^++0 event above the cutoff (and vice versa, some W^++1 events below the cutoff) is an effect of the added cascade. The effect of the cutoffs is not completely invisible, however, as is clear in figure 3d, where we enhance the effect by showing the ratio of $p_\perp$-spectra of ME1PS and ARIADNE for the different cutoffs.

We can now proceed with some confidence to investigate our new algorithm also for higher parton multiplicities in the MEG. Here we will, of course, expect differences w.r.t. ARIADNE. These differences would be the ones desired from replacement of the products of splitting functions with the exact tree-level matrix elements, and also from the additional processes not present in the dipole cascade, such as the one in figure 2. For small scales, these differences should be small and we would still like to have a smooth behavior of any observable sensitive to the cutoff used in MADGRAPH, at least for small enough E_{cut}. There may also be differences arising from deficiencies in our algorithm, since there are now additional construction steps possible.

In figure 4a we again show the W^+ $p_\perp$ spectrum, but now using ME4PS and comparing with ARIADNE and also with the default PYTHIA parton shower (which also includes a tree-level matrix element correction for the first emission). We find that there is now an increase

[3]In fact we discovered a small bug in the default ARIADNE treatment, related to a mismatch between the invariant $p_\perp$and the actual transverse momentum in gluon emissions. This bug has been fixed in the latest release of ARIADNE.

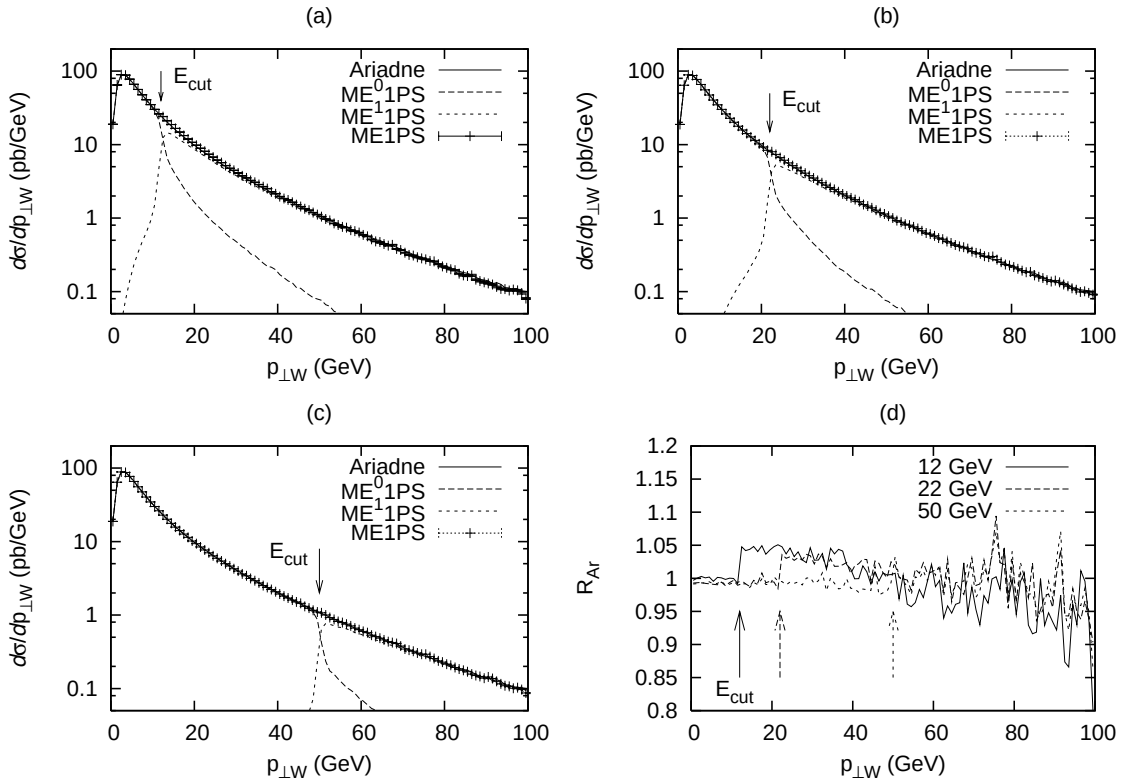

Figure 3: Differential cross section as a function of transverse momentum of the W for standard ARIADNE compared to the first order matrix element correction for the different cutoffs (a) 12 GeV, (b) 22 GeV and (c) 50 GeV. In all cases the full line is standard ARIADNE while the error bars shows the results from ME1PS. The long-dashed and short-dashed lines indicate the contributions from W+0jet and W+1jet matrix elements to ME1PS respectively. Plot (d) shows the ratio between the ME1PS distributions and standard ARIADNE for cutoffs of 12 GeV (full line), 22 GeV (long-dashed line) and 50 GeV (short-dashed line).

at large $p_\perp$ for the ME4PS case, which is attributed to the desired higher-order effects. We note that there is still no dramatic discontinuity around the cutoff.

There is distinct difference in the small-$p_\perp$ behavior for the PYTHIA distribution. The peak in PYTHIA is shifted towards smaller $p_\perp$, as compared to ARIADNE, with or without the new matching algorithm. This is a known problem with PYTHIA, which need an uncomfortably large intrinsic transverse momentum of the proton to reproduce data. This is shown in more detail in figure 4b where we focus on the small-$p_\perp$ part of the spectrum and where we have two curves for PYTHIA, one with an average squared intrinsic transverse momentum, $\langle k_{\perp i}^2 \rangle$, of 1 GeV^2 and one with 4 GeV^2. Note that also ARIADNE has an intrinsic transverse momentum, but this is at a typical non-perturbative value of $\langle k_{\perp i}^2 \rangle = 0.36$ GeV^2, but the increased possibility of radiating gluons in the dipole cascade, especially in the direction of the remnants, will give the slightly harder $p_\perp$ spectrum. From reference [52] we know that PYTHIA can only describe data with the higher intrinsic transverse momentum[4],

[4]In later PYTHIA releases the higher value is the default.

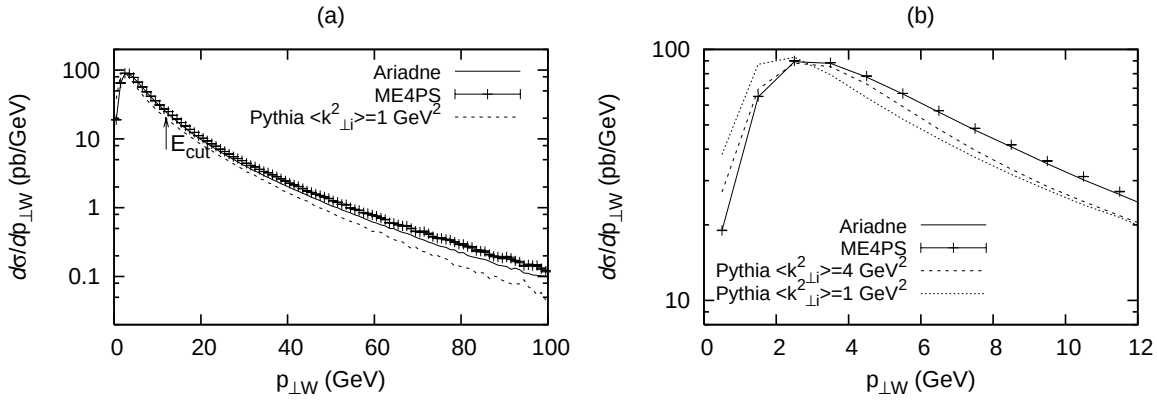

Figure 4: (a) Differential cross section as a function of transverse momentum of the W for standard ARIADNE (full line), ARIADNE with up to fourth order matrix element corrections (error bars) and PYTHIA with intrinsic transverse momentum of $\langle k_\perp^2 \rangle = 1$ GeV^2 (short-dashed line). (b) is the same concentrating on the small $p_{\perp W}$ region, where also PYTHIA with intrinsic transverse momentum of $\langle k_\perp^2 \rangle = 4$ GeV^2 is shown (dotted line).

which is quite close to ARIADNE [5] in figure 4. Also other DGLAP-based parton showers need a high intrinsic transverse momentum to describe Tevatron data (HERWIG: $\langle k_\perp^2 \rangle \approx 2.6$ GeV^2 [53], APACIC++/SHERPA [6]: $\langle k_\perp^2 \rangle \approx 1.3$ GeV^2 [7]), although not as high as PYTHIA, a value above one GeV^2 is needed and well above what is required in ARIADNE.

There is still a difference in shape and with the increased statistics collected in Tevatron Run II, it may be possible to distinguish between the two.

Next we want to check the cutoff sensitivity also for higher jet rates. We do that by taking the final events on parton level and cluster them with the same $k_\perp$-algorithm which was used for the regularization in MADGRAPH, and then look at what value of the resolution variable, d_n, an event is clustered from n-jets to $n-1$-jets. In figure 5 we show such distributions for $n = 1, 2, 3$ and 4 for $E_{\rm cut} = 12$ GeV, where d_3 and d_4 are only plotted for values up to 50 GeV due to limited statistics. We also show the individual contributions from different parton multiplicities delivered by MADGRAPH. We see that there is a clear difference between ME4PS and ARIADNE for large d_n values, which is expected from the improved treatment of events with several hard jets. We note that there is a rather smooth transition across $E_{\rm cut}$. In figure 6 we also show results for $E_{\rm cut} = 22$ and 50 GeV, now presented as ratios between ME4PS and ARIADNE. As expected we here see more clearly where the new matrix element treatment sets in above $E_{\rm cut}$. In figure 6 we also show the ratio between PYTHIA and ARIADNE and we find that, as compared to the effects of the matrix element corrections, the difference between the two cascades is small.

Next we want to see if the features of the ARIADNE resummation are reflected in our new algorithm. As noted before, the emission of gluons are allowed in a larger phase

[5] We have not compared directly with Tevatron results here due to uncertainties about the corrections made to the data.

[6] APACIC++/SHERPA uses a Gaussian distribution with a width of 0.8 GeV, but centered around 0.8 GeV, while the other programs use a Gaussian centered around zero.

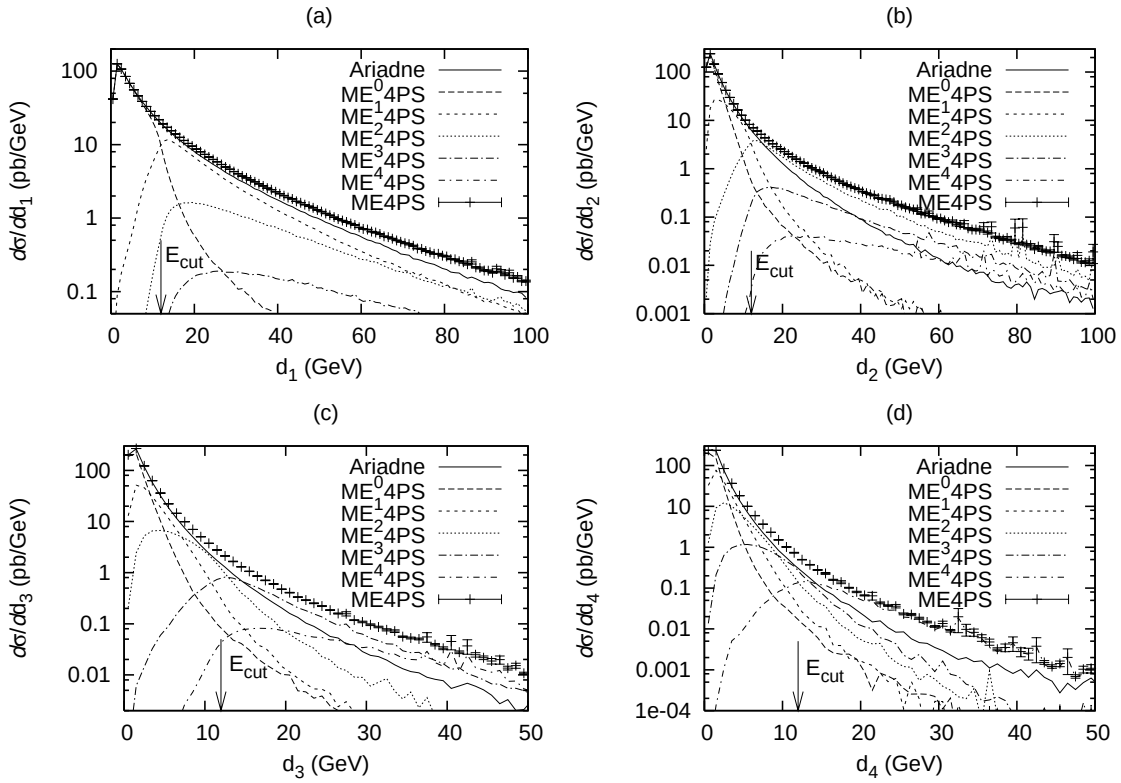

Figure 5: Differential cross section as a function of the scale where the jets merge in the $k_\perp$-algorithm, where d_i denotes the scale when i jets merge into $i-1$ jets. Figures (a), (b), (c) and (d) shows d_1, d_2, d_3 and d_4 respectively. In all cases the error bars show the results from ARIADNE corrected with up to fourth order matrix elements (ME4PS), while the contributions from W+0jet, W+1jet,..., W+4jets matrix elements are shown with long-dashed, short-dashed, dotted, lond-dash-dotted and sort-dash-dotted lines respectively. Also shown are the results from standard ARIADNE (full line).

space region in ARIADNE as compared to a conventional PSEG, hence the no-emission probabilities should be affected. Also, in a conventional DGLAP-based initial-state PSEG, the parton closest to the W is also the hardest one. This is not the case for ARIADNE where, effectively, contributions of emissions with lower $p_\perp$ between the hardest parton and the W is taken into account, as illustrated in figure 7a. Possible BFKL effects in similar situations has previously been investigated in [54]. One observable which may be sensitive to this difference is the pseudorapidity difference between the W and a jet, $\Delta\eta_{\mathrm{W}j}$, which then should be enhanced for large $\Delta\eta_{\mathrm{W}j}$ in ARIADNE as compared to PYTHIA. This is also the case as shown in figure 7b. Of course, the exact tree-level matrix element will also contain contributions such as the one in 7a, and we see that the enhancement at large $\Delta\eta_{\mathrm{W}j}$ is even more significant, when ME corrections are added to ARIADNE with low enough cutoff. For higher cutoffs there will, of course, be much fewer events of this type generated by the MEG. It would be interesting to see if including CKKW corrections also in PYTHIA would bring it closer to ARIADNE and ME4PS. This could be expected since including higher order corrections could in the end make things more insensitive to the particular kind of

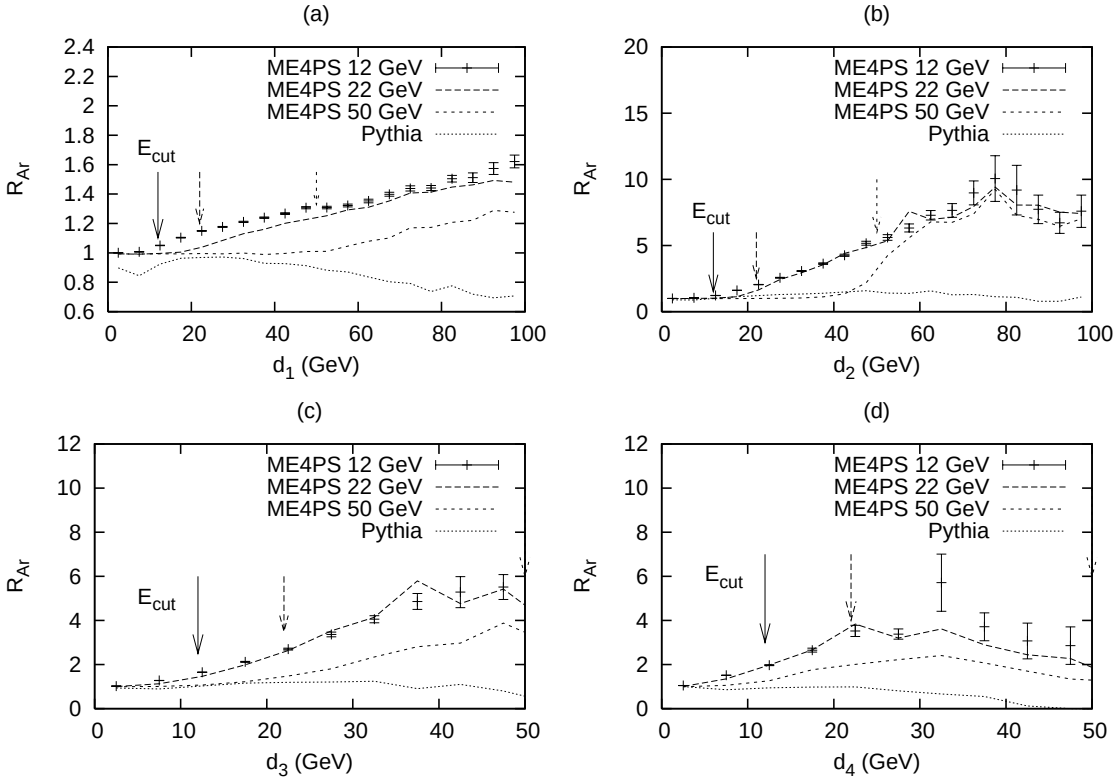

Figure 6: Distributions in jet merging scales, d_i, given as ratios w.r.t. standard ARIADNE. Figures (a), (b), (c) and (d) shows d_1, d_2, d_3 and d_4 respectively. The ME-corrected ARIADNE (ME4PS) is shown for cutoffs of 12 GeV (error bars), 22 GeV (long-dashed line) and 50 GeV (short-dashed line). Also shown is the results for PYTHIA (dotted line).

resummation used.

One of the advantages of the matrix element corrections is that correlations between hard partons are more accurately described. This may be important when eg. estimating backgrounds to different searches. We will here consider the background to top production at the Tevatron for the semi-leptonic channel which corresponds to W+4-jets. In a realistic top search one would use identified b-jets, but since our MADGRAPH events do not include b-quarks we look at W+4-jets in general.

In figure 8 we show the W+4-jets background to the top-mass distribution. We obtained it by using the $k_\perp$-algorithm to cluster four jets and required that the jet scale was above 12 GeV. Form these we found the two jets j_1 and j_2 with an invariant mass m_{12} closest to the W mass. If no jets with $|m_{12} - m_{\mathrm{W}}| < 20$ GeV were found, the event was rejected. Then we selected a third jet, j_3, so that the difference $|m_{123} - m_{\mathrm{W}4}|$ was minimized, where m_{123} is the invariant mass of jets 1, 2 and 3, and $m_{\mathrm{W}4}$ is the invariant mass of the $\mathrm{W}^+$and jet 4. If the difference $|m_{123} - m_{\mathrm{W}4}| < 20$ GeV then the event was accepted and the constructed top mass is defined as the average of m_{123} and $m_{\mathrm{W}4}$. Clearly the total cross section would be underestimated by the leading-order predictions of PYTHIA and ARIADNE. In figure 8 we therefore only show the normalized shape and find that

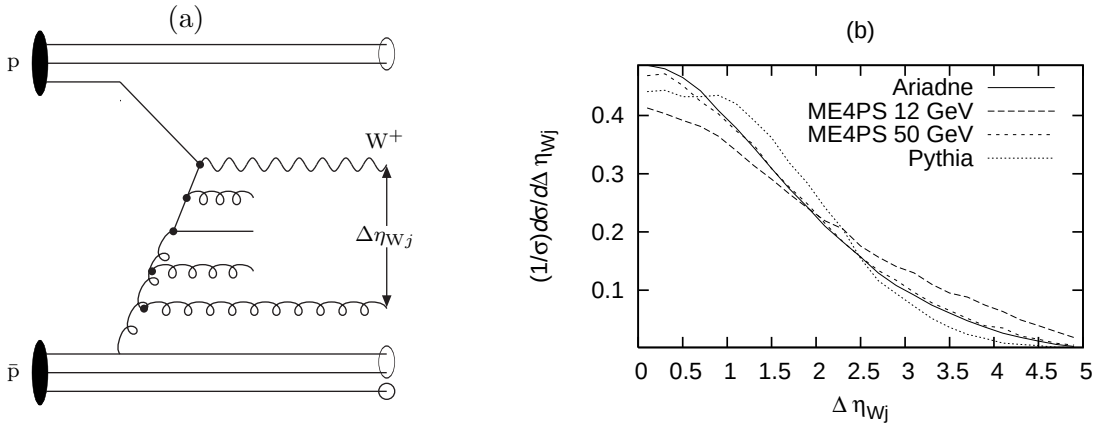

Figure 7: Part (a) shows a typical diagram contributing to the pseudorapidity difference between the W and the hardest jet. Diagrams with soft jets between the W and the hardest jet can not be generated through DGLAP evolution, but are included in the matrix element corrections. Plot (b) is a normalized distribution of the difference in pseudorapidity between the hardest jet and the W, where the jet is defined using the $k_\perp$-algorithm with a 12 GeV cutoff and the hardest jet has a transverse momentum greater than 40 GeV. The distribution is shown for ARIADNE (full line), PYTHIA (dotted line), and ME4PS with a 12 GeV and 50 GeV cutoff (long- and short-dashed lines respectively).

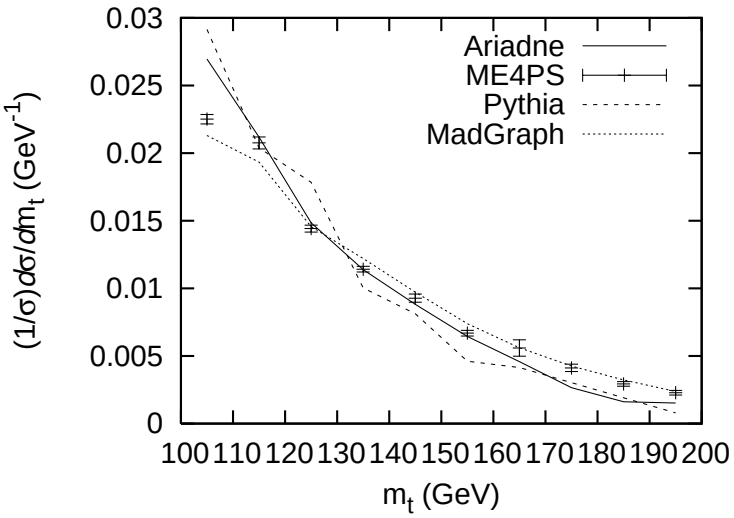

Figure 8: The normalized differential cross section given as a function of the reconstructed top quark mass for ARIADNE (full line), PYTHIA (short-dashed line), and ME4PS with 12 GeV cutoff (long-dashed with error bars). Also shown is the results from the pure tree-level matrix element without parton showers added using a 12 GeV cutoff (dotted line).

PYTHIA and ARIADNE are quite similar and that no significant change is introduced by the matrix element correction to ARIADNE. We also show the result from using the tree-level 4-jet matrix elements directly, without reweighting and adding a cascade. We find no large differences, although there is a tendency for the parton shower results to overshoot the pure matrix element result for small m_t and undershoot for large m_t. We also see that

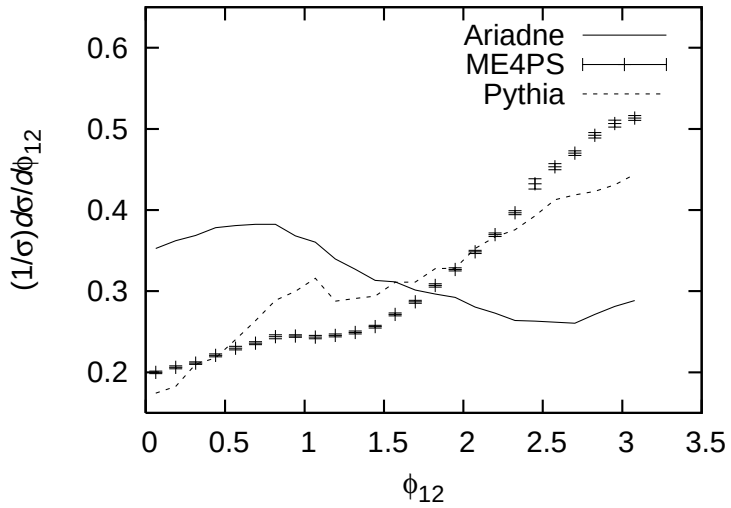

Figure 9: Normalized distribution of the azimuthal angle difference between the two hardest jets defined using the $k_\perp$-algorithm with a 12 GeV cutoff. The distribution is shown with standard ARIADNE (full line), PYTHIA (short-dashed line), and ME4PS with 12 GeV cutoff (error bars).

ARIADNE with matrix element corrections agree with the pure matrix elements for large m_t, while for small m_t it is slightly closer to the parton shower results.

To focus more specifically on angular correlations, we finally look at the azimuthal angle between the two hardest jets, ϕ_{12}. This observable is important for understanding how higher order emissions influence the transverse momentum of the W, $p_{\perp \mathrm{W}}$. For $\phi_{12} \sim \pi$, the emission of a second jet decreases the $p_{\perp \mathrm{W}}$, while for $\phi_{12} \sim 0$ the $p_{\perp \mathrm{W}}$ is increased. In ARIADNE, after a first emission of a gluon, a second gluon will be radiated isotropically in azimuth in the rest system of the radiating dipole. Since this dipole is boosted in the direction of the first gluon, we expect that the second gluon is more likely to go in the same direction. This is not true for PYTHIA, where successive initial-state emissions are uncorrelated in azimuth (with the recoils, the net effect is a bias towards large ϕ_{12}). In figure 9 we see the (normalized) ϕ_{12} distributions, and indeed we find that ARIADNE is more biased towards $\phi_{12} \sim 0$. Adding matrix element corrections removes this bias and brings the distribution closer to the PYTHIA result. Hence this indicates that the azimuthal correlations in standard ARIADNE are not very well modeled.

6. Conclusions

We have presented a way to implement a CKKW procedure for combining events generated according to tree-level matrix elements for W-production with the dipole cascade of ARIADNE. Although the basic principles are fairly simple, the details of our procedure is rather involved, which is mandated by our aim to become as insensitive as possible to the cutoff needed in the matrix element generation.

Our strategy is to take any partonic state generated by a MEG and try to find a likely history of emissions which ARIADNE would have performed in order to generate this

state. Rather than just using the constructed emission scales to calculate analytic Sudakov form factors to reweight the states, as is done in the original CKKW procedure, we find exactly the Sudakov form factors ARIADNE would have used. In addition we reweight the states with the parton densities functions and the so-called soft suppression function which ARIADNE would have used.

The PDF reweighting means that the overall normalization of cross sections are still given by the leading order diagrams used by standard ARIADNE. However, we expect an improvement of the shapes of final state distributions as compared to the standard parton shower description.

We have presented several investigations into how the ARIADNE program is improved by adding matrix element corrections. In some cases we also compared to the PYTHIA parton shower to get some insight into how well these standard cascade programs reproduces higher order matrix elements.

In one case we looked at the azimuthal correlation between the two hardest jets, and found that the difference between ARIADNE and PYTHIA was large. When corrected with matrix elements, ARIADNE came much closer to PYTHIA, indicating that such azimuthal correlations are not handled very well in standard ARIADNE.

In our quasi-realistic top-background observable we found that ARIADNE and PYTHIA were quite close and that no drastic effect was obtained by including matrix element corrections.

For the W–jet rapidity correlation we again found clear differences between ARIADNE and PYTHIA, and that these were even enhanced when correcting ARIADNE with matrix elements. This indicates that such correlations are not very well described by PYTHIA, while standard ARIADNE does a better job, although it can be improved.

We believe that the rapidity correlations indicate that non-ordered evolution is of importance for W-production at the Tevatron. Such evolution is expected to be important in small-x processes, and the fact that it shows up here, where $x \sim m_W/\sqrt{S} \approx 0.04$, may be somewhat surprising. We also believe that the inclusion of non-ordered evolution is why ARIADNE is able to reproduce experimental data on the small-$p_\perp$-distribution of the W and Z^0, distributions which can only be described by PYTHIA if an uncomfortably large intrinsic transverse momentum is added.

The fact that matrix element corrections can give us hints about where unordered evolutions may become important, is an indication that it would be very interesting to implement CKKW also for DIS[7] and compare with HERA data. Also, at the LHC where W-production may be argued to be a true small-x process ($x \sim m_W/\sqrt{S} \lesssim 0.006$), it should be interesting to study matrix element corrections. In fact also Higgs production at the LHC may be considered to be a small-x process. We will come back to these processes in future publications.

Acknowledgments

We would like to thank Stephen Mrenna, Peter Richardson, Torbjörn Sjöstrand and

[7]Preliminary results for DIS have already been presented in [56].

Christoffer Åberg for useful discussions. Special thanks to Stephen Mrenna for supplying us with event files generated with MadGraph/MadEvent.

References

[1] S. Catani, F. Krauss, R. Kuhn, and B. R. Webber *JHEP* **11** (2001) 063, hep-ph/0109231.

[2] L. Lönnblad *JHEP* **05** (2002) 046, hep-ph/0112284.

[3] G. Gustafson and U. Pettersson *Nucl. Phys.* **B306** (1988) 746.

[4] G. Gustafson *Phys. Lett.* **B175** (1986) 453.

[5] L. Lönnblad *Comput. Phys. Commun.* **71** (1992) 15–31.

[6] F. Krauss *JHEP* **08** (2002) 015, hep-ph/0205283.

[7] F. Krauss, A. Schalicke, S. Schumann, and G. Soff *Phys. Rev.* **D70** (2004) 114009, hep-ph/0409106.

[8] F. Krauss, A. Schaelicke, S. Schumann, and G. Soff hep-ph/0503280.

[9] S. Mrenna and P. Richardson *JHEP* **05** (2004) 040, hep-ph/0312274.

[10] M. Mangano, "The so-called MLM prescription for ME/PS matching." http://www-cpd.fnal.gov/personal/mrenna/tuning/nov2002/mlm.pdf. Talk presented at the Fermilab ME/MC Tuning Workshop, October 4, 2002.

[11] M. L. Mangano, M. Moretti, and R. Pittau *Nucl. Phys.* **B632** (2002) 343–362, hep-ph/0108069.

[12] B. Andersson, G. Gustafson, L. Lönnblad, and U. Pettersson *Z. Phys.* **C43** (1989) 625.

[13] L. Lönnblad *Nucl. Phys.* **B458** (1996) 215–230, hep-ph/9508261.

[14] T. Sjöstrand, L. Lönnblad, and S. Mrenna, "PYTHIA 6.2: Physics and manual," arXiv:hep-ph/0108264.

[15] M. Bengtsson and T. Sjöstrand *Z. Phys.* **C37** (1988) 465.

[16] G. Corcella *et al. JHEP* **01** (2001) 010, hep-ph/0011363.

[17] T. Gleisberg *et al. JHEP* **02** (2004) 056, hep-ph/0311263.

[18] F. Krauss, A. Schalicke, and G. Soff hep-ph/0503087.

[19] V. N. Gribov and L. N. Lipatov *Yad. Fiz.* **15** (1972) 781–807.

[20] L. N. Lipatov *Sov. J. Nucl. Phys.* **20** (1975) 94–102.

[21] G. Altarelli and G. Parisi *Nucl. Phys.* **B126** (1977) 298.

[22] Y. L. Dokshitzer *Sov. Phys. JETP* **46** (1977) 641–653.

[23] E. A. Kuraev, L. N. Lipatov, and V. S. Fadin *Sov. Phys. JETP* **44** (1976) 443–450.

[24] E. A. Kuraev, L. N. Lipatov, and V. S. Fadin *Sov. Phys. JETP* **45** (1977) 199–204.

[25] I. I. Balitsky and L. N. Lipatov *Sov. J. Nucl. Phys.* **28** (1978) 822–829.

[26] M. Ciafaloni *Nucl. Phys.* **B296** (1988) 49.

[27] S. Catani, F. Fiorani, and G. Marchesini *Phys. Lett.* **B234** (1990) 339.

[28] S. Catani, F. Fiorani, and G. Marchesini *Nucl. Phys.* **B336** (1990) 18.

[29] G. Marchesini *Nucl. Phys.* **B445** (1995) 49–80, hep-ph/9412327.

[30] M. Bengtsson and T. Sjostrand *Phys. Lett.* **B185** (1987) 435.

[31] M. Bengtsson and T. Sjöstrand *Nucl. Phys.* **B289** (1987) 810.

[32] M. H. Seymour *Nucl. Phys.* **B436** (1995) 443–460, hep-ph/9410244.

[33] M. H. Seymour *Comp. Phys. Commun.* **90** (1995) 95–101, hep-ph/9410414.

[34] M. H. Seymour, "Matrix element corrections to parton shower simulation of deep inelastic scattering." Contributed to 27th International Conference on High Energy Physics (ICHEP), Glasgow, Scotland, 20-27 Jul 1994.

[35] L. Lönnblad *Z. Phys.* **C65** (1995) 285–292.

[36] G. Miu and T. Sjöstrand *Phys. Lett.* **B449** (1999) 313–320, hep-ph/9812455.

[37] S. Mrenna, "Higher order corrections to parton showering from resummation calculations," hep-ph/9902471.

[38] G. Corcella and M. H. Seymour *Nucl. Phys.* **B565** (2000) 227–244, hep-ph/9908388.

[39] Y. L. Dokshitzer. in *Workshop on Jet studies at LEP and HERA*, Durham 1990, see *J. Phys.* **G17** (1991) 1572ff.

[40] S. Catani, Y. L. Dokshitzer, M. Olsson, G. Turnock, and B. R. Webber *Phys. Lett.* **B269** (1991) 432–438.

[41] S. Catani, Y. L. Dokshitzer, M. H. Seymour, and B. R. Webber *Nucl. Phys.* **B406** (1993) 187–224.

[42] L. Lönnblad *Z. Phys.* **C58** (1993) 471–478.

[43] S. Moretti, L. Lönnblad, and T. Sjöstrand *JHEP* **08** (1998) 001, hep-ph/9804296.

[44] B. Andersson, G. Gustafson, and L. Lönnblad *Nucl. Phys.* **B339** (1990) 393–406.

[45] K. Hamacher and M. Weierstall hep-ex/9511011.

[46] N. Brook, R. G. Waugh, T. Carli, R. Mohr, and M. Sutton. Prepared for Workshop on Future Physics at HERA (Preceded by meetings 25-26 Sep 1995 and 7-9 Feb 1996 at DESY), Hamburg, Germany, 30-31 May 1996.

[47] E. Boos *et al.* hep-ph/0109068.

[48] A. Schaelicke and F. Krauss hep-ph/0503281.

[49] N. Lavesson, L. Lönnblad, and C. Åberg. Preprint in preparation.

[50] F. Maltoni and T. Stelzer *JHEP* **02** (2003) 027, hep-ph/0208156.

[51] J. Pumplin *et al. JHEP* **07** (2002) 012, hep-ph/0201195.

[52] E. Thome hep-ph/0401121.

[53] E. L. Nurse. FERMILAB-THESIS-2005-05.

[54] J. R. Andersen, V. Del Duca, F. Maltoni, and W. J. Stirling *JHEP* **05** (2001) 048, hep-ph/0105146.

[55] S. Frixione and B. R. Webber *JHEP* **06** (2002) 029, hep-ph/0204244.

[56] C. Åberg, "Correcting the Colour Dipole Cascade with Fixed Order Matrix Elements in Deep Inelastic Scattering." Diploma thesis, LU-TP 04-25.

A. Appendix: Construction

Here we describe in some detail the different kinds of steps possible when constructing intermediate partonic states from events generated by a MEG. In figure 10 the different steps are shown schematically.

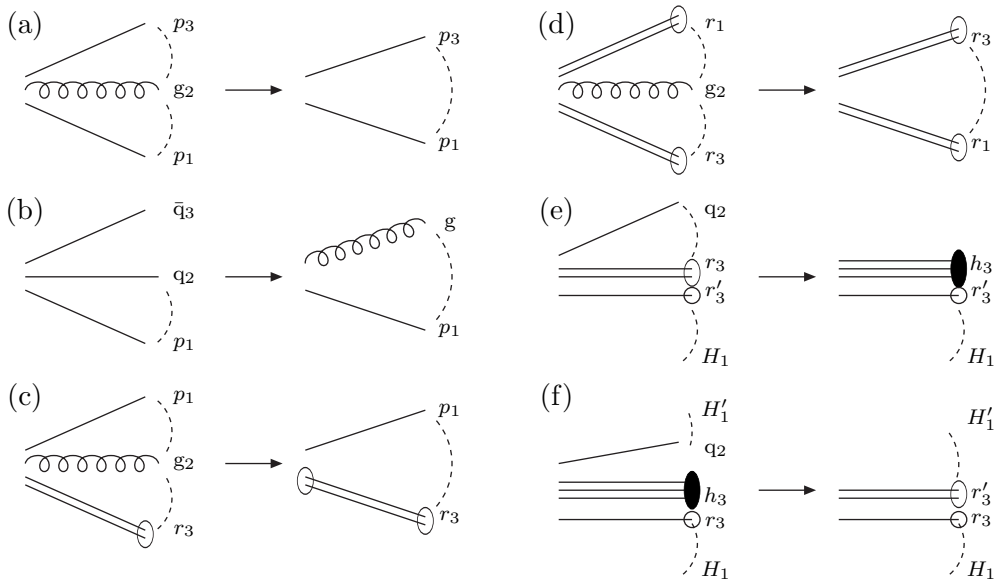

Figure 10: Symbolic pictures of possible steps which are possible when constructing possible intermediate partonic states from events generated by a MEG. The different possibilities are described in the text. The dashed lines indicate colour-connections.

(a) p_1–g$_2$–$p_3 \longrightarrow p_1$–p_3: A gluon, colour-connected to two non-remnant partons, p_1 and p_3, is constructed to a single dipole between p_1 and p_3. The splitting function is given by one of eqs. (3.4) – (3.6) depending on whether p_1 and p_3 are gluons or quarks. The scale is given by the invariant $p_\perp$ in eq. (3.1). No PDF ratio is relevant. In the rest frame of the construction, p_1 will retain its direction if it is a gluon and p_3 is a quark, and vice versa. If both p_1 and p_3 are gluons or both are quarks, the direction of p_1 is rotated away from the original p_3 direction with an angle $\beta x_1^2/(x_1^2 + x_3^2)$, where β is the original angle between p_1 and p_3. This corresponds to the standard recoil treatment for gluon emission in ARIADNE.

(b) p_1–q$_2$ $\bar{\text{q}}_3 \longrightarrow p_1$–g. A q$\bar{\text{q}}$-pair is constructed into a gluon as long as they are each others anti-particles, are connected to different strings, and the end-points of these strings are not remnants of the same incoming hadron. The splitting function is given by eq. (3.8). The scale is given by the invariant $p_\perp$ in eq. (3.1). No PDF ratio is relevant. In the rest system of the construction, p_1 will retain its direction.

(c) p_1–g$_2$–$r_3 \longrightarrow p_1$–r_3: A gluon, colour-connected to one remnant, r_3 and one non-remnant parton, p_1, is constructed to a single dipole between p_1 and r_3. The splitting function is given by eqs. (3.4) or (3.5) depending on whether p_1 is a quark or a gluon. If r_3 is one of two remnants of the same hadron (this corresponds to an extracted gluon), the PDF ratio is taken to be Θ, otherwise it is Θ/z. If a W is present in the event and it is *close* to g$_2$, the transverse momentum of the gluon in the center of mass system of p_1 and r_3 is given to the W, and the longitudinal momentum is absorbed by p_1 and r_3. The scale is given by the invariant $p_\perp$ in eq. (3.1) (calculated as if no W was close, ie. the transverse momenta of the gluon is transfered to p_1 and r_3 with the weight $x_i^2/(x_1^2 + x_3^2)$). Here *close* means that $p_{+g} < p_{+\text{W}}$ and $p_{-g} < p_{-\text{W}}$,

where $p_{\pm W}$ is calculated for the constructed W momenta. If there is no W close by the momentum of the gluon is shared by p_1 and r_3, where r_3 retains its direction. The scale is given by the invariant $p_\perp$.

(d) $r_1{-}\mathrm{g}_2{-}r_3 \longrightarrow r_1{-}r_3$: A gluon connected to two remnants, one from each incoming hadron, is constructed to a single dipole between the remnants. The splitting function is given by eqs. (3.4). When calculating the scale a fraction $x_i^2/(x_1^2 + x_3^2)$ of the transverse momenta from the gluon is transfered to each of the remnants and the scale is given by the invariant $p_\perp$ in eq. (3.1). The PDF ratio is given by the product of the Θ on each side, divided by z if the corresponding remnant is not one of two remnants of the same hadron. The transverse momentum of the gluon is transfered to the W if one is present, otherwise it is transfered to the hard subsystem containing the rest of the non-remnant partons in the event. The longitudinal momentum is divided between r_1 and r_3.

(e) $H_1\ r_3'\ \mathrm{q}_2{-}r_3 \longrightarrow H_1\ r_3'\ h_3$: This corresponds to the inverse of an initial-sate $\mathrm{g} \to \mathrm{q}$ splitting. For a quark, q_2, connected to a remnant, r_3, and a hard subsystem, H_1 (which contains the W if present), connected to another remnant, r_3', from the same incoming hadron and arising from the extraction of a corresponding anti-quark, $\bar{\mathrm{q}}'$, a hadron, h_3, is formed from q_2 and r_3. The splitting function is the standard Altarelli–Parisi one, $P_{\mathrm{g}\to\mathrm{q}}(z)$. The scale is the squared transverse momentum of q_2 in the rest frame of the event. The PDF ratio is the same as would have been used in a conventional parton shower. The transverse momentum of q_2 is transfered to H_1, and the longitudinal momentum is shared between H_1, r_3' and h_3. The relative sharing of longitudinal momenta between r_3' and h_3 is the same as for the original r_3' and r_3.

(f) $H_1\ \mathrm{q}_2\ r_3\,(h_3) \longrightarrow H_1\ r_3\ r_3'$: A quark, q_2, which may have been extracted from a hadron resulting in a remnant r_3 may be absorbed into a the remnant, constructing an initial-state $\mathrm{q} \to \mathrm{g}$ splitting. The remnant is split into two, possibly together with a remnant hadron, h_3, if q_2 was a sea-quark. The splitting function is the standard Altarelli–Parisi one, $P_{\mathrm{q}\to\mathrm{g}}(z)$. The scale is the squared transverse momentum of q_2 in the rest frame of the event. The PDF ratio is the same as would have been used in a conventional parton shower. The transverse momentum of q_2 is transfered to the spectator hard subsystem, H_1, and the longitudinal momentum is shared between H_1, r_3 and r_3'. The relative sharing of longitudinal momenta between r_3 and r_3' is the same as for the original r_3 and h_3 if h_3 was present, otherwise the momenta is shared as is normally done in ARIADNE when a gluon is extracted from a hadron. Note that there is no corresponding emission in ARIADNE.